Catena 86 (2011) 98–109

Contents lists available at ScienceDirect

Catena

journal homepage: www.elsevier.com/locate/catena

Controls of infiltration–runoff processes in Mediterranean karst rangelands in SE Spain

Xiao-Yan Li [a,b,*], Sergio Contreras [b,c], Albert Solé-Benet [b], Yolanda Cantón [d], Francisco Domingo [b,e], Roberto Lázaro [b], Henry Lin [f], Bas Van Wesemael [g], Juan Puigdefábregas [b]

[a] State Key Laboratory of Earth Surface Processes and Resource Ecology, Beijing Normal University, Beijing 100875, China
[b] Estación Experimental de Zonas Áridas, Consejo Superior de Investigaciones Científicas, Carretera de Sacramento s/n, La Cañada de San Urbano, 04120 Almería, Spain
[c] Centro de Edafología y Biología Aplicada del Segura, Consejo Superior de Investigaciones Científicas, Campus Universitario de Espinardo, 30100 Murcia, Spain
[d] Departamento de Edafología y Química Agrícola, Escuela Politécnica Superior, Universidad de Almería, 04120 Almería, Spain
[e] Departamento de Biología Vegetal y Ecología, Escuela Politécnica Superior, Universidad de Almería, 04120 Almería, Spain
[f] Dep. of Crop and Soil Sciences, 116 ASI Building, The Pennsylvania State Univ., University Park, PA 16802, USA
[g] George Lemaître Centre for Earth and Climate Research, Earth and Life Institute, Université Catholique de Louvain, 1348 Louvain-la-Neuve, Belgium

ARTICLE INFO

Article history:
Received 24 November 2010
Received in revised form 18 February 2011
Accepted 1 March 2011

Keywords:
Soil surface properties
Vegetation
Rock outcrop
Rock fragments
Antecedent soil moisture
Karst

ABSTRACT

Semiarid karst landscapes represent an important ecosystem surrounding the Mediterranean Basin for which little is known on runoff generation. Knowledge of the sources and patterns of variation in infiltration–runoff processes and their controls is important for understanding and modelling the hydrological functions of such ecosystems. The objectives of this paper are to determine the infiltration rates and their controls in a representative mountain karst area (Sierra de Gádor, SE Spain) at micro-plots and to investigate the integrated response of rainfall on a typical hillslope. Rainfall simulations in micro-plots and natural rainfall-runoff monitoring on a hillslope were carried out complementarily. We investigated the role of soil surface components (vegetation, rock outcrop, fracture, and soil crust), topographic position, antecedent soil moisture, and rainfall characteristics in regulating infiltration–runoff processes. Results of rainfall simulation revealed the importance of vegetation cover and the presence of rock fractures in promoting the infiltration in the limestone karst landscape, while bare patches and rock outcrops acted as sources for runoff. All plots with >50% vegetation cover had no runoff with up to 55 mm h^{-1} of simulated rain. In contrast, nearly all bare plots had runoff under the same simulated rain, with runoff coefficients ranging from 3.1 to 20.6% on dry soil surface conditions, and from 2.0 to 65.4% on wet soil surfaces. Runoff coefficients amounted to 59.0–79.5% for rock outcrops without cracks, but were drastically reduced by the presence of cracks. The surfaces with rock fragments resting on the soil (generally located in the middle of the slopes) prevented more effectively the runoff generation than those surfaces where rock fragments were embedded in the top soil. Antecedent soil moisture had significant impact on runoff generation, with wet soil having doubled runoff coefficient, shortened time to runoff, and increased runoff rate compared to the same but dry soil. Linear regressions indicated that the main controls for constant infiltration rate were the cover percentages of vegetation and litter, plus rainfall intensity; while the major controls for runoff coefficient were the bare soil and vegetation coverage, plus rainfall intensity. High infiltration rates measured at the micro-plots agreed with low intra-event runoff coefficients (mostly below 1%) observed under natural rainfalls at the hillslope. Runoff depth and coefficient at the hillslope was significantly correlated with rainfall depth, maximum hourly rainfall intensity and antecedent precipitation over 20 days (AP_{20}). During the 1.5-year monitoring period from Sep-2003 to Mar-2005, the overall infiltration was 41% of the total rainfall amount and the maximum infiltration rate was almost 94% of the largest single rainfall event. The results from this study contribute to improved understanding of the magnitude and controls of the surface runoff in semiarid karst mountain areas.

1. Introduction

Hydrological processes in semiarid areas, such as infiltration and runoff are highly variable in space and time. Knowledge of the sources and patterns of variation in these processes and their controlling factors is crucial for understanding and modelling the hydrological functioning of semiarid ecosystems (Mayor et al., 2009). Previous

* Corresponding author at: State Key Laboratory of Earth Surface Processes and Resource Ecology, Beijing Normal University, Xinjiekouwai Street 19, Beijing, 100875, China. Tel.: +86 10 58802716; fax: +86 10 58802716.
E-mail address: xyli@bnu.edu.cn (X.-Y. Li).

0341-8162/$ – see front matter © 2011 Elsevier B.V. All rights reserved.
doi:10.1016/j.catena.2011.03.003

studies have demonstrated that semiarid Mediterranean slopes behave as a mosaic of runoff generation and infiltration patches (Yair and Lavee, 1985; Yair, 1996; Lavee et al., 1991) depending strongly on the morphometric characteristics of the slopes, the lithology, the land use and the different development of soils and their cover (Yair and Lavee, 1985; Abrahams and Parsons, 1991; Solé-Benet et al., 1997; Cantón et al., 2002; Calvo-Cases et al., 2003). Although it is well-known that surface types and soil properties, such as vegetation type and cover, rock fragment cover, crust cover, soil organic carbon content, and soil depth, among others, can affect infiltration–runoff processes (Wilcox et al., 1988; Solé-Benet et al., 1997; Calvo-Cases et al., 2003), their interaction and relative importance in driving the hydrological behaviour remains unclear (Seeger, 2007; Mayor et al., 2009).

Karst landscapes, areas in which dissolution of bedrock is one of the dominant geomorphic processes, occupy 10–20% of the earth (Palmer, 1991). Although extensive areas of carbonate and karst terrains exist in subhumid and semiarid landscapes, we know relatively little about how runoff is generated in these landscapes (Wilcox et al., 2007). Limestone and other carbonate rocks often display solution features and/or fractures that facilitate subsurface flow of water (Palmer, 1991; Wilcox et al., 2007). Runoff generation has been found to be especially complex on rangelands underlain by limestone bedrock (Wilcox et al., 2006), and are assumed to be generated by infiltration excess, saturation excess from subsurface layers, or a combination of both types (e.g. Calvo-Cases et al., 2003; Wilcox et al., 2006). A review by Calvo-Cases et al. (2003) of 37 sites located in Mediterranean limestone areas showed that soil infiltration was usually high (8 to >100 mm h^{-1}) in these landscapes, and event-based runoff coefficients ranged from 0.2% to 80%.

Semiarid limestone and dolomite karst landscapes are common ecosystems surrounding the Mediterranean Basin (Calaforra, 2004). On a local scale, these landscapes are frequently used for seasonal grazing. On a regional scale, they are the main recharge areas for important coastal aquifers which supply freshwater resources for drinking, agriculture and other human activities. In general, the supply of water for grazing is of major concern in these areas because surface water is scarce and usually restricted to springs on the geological contacts between carbonated and impermeable lithologies.

The Sierra de Gádor Mountains, located in southeast Spain, have a karst landscape consisting of a thick series of Triassic carbonate rocks (limestones and dolomites) which recharge the deep aquifers of Campo de Dalías, a coastal plain with a highly profitable horticulture and tourist industry. Water demand has rapidly increased in this coastal area due to tourism and expansion of intensive agriculture, consequently increasing the dependence on groundwater resources. Because of the secondary porosity characterising karst landscapes, soil infiltration rates in the Sierra de Gádor are assumed to be high. However, no specific data are available. This requires a better understanding of infiltration–runoff processes and their relationship to surface characteristics, landscape attributes and geologic properties. One of the main geomorphologic units in the Sierra de Gádor is a relatively flat area developed extending from 1400 to 1800 m.a.s.l. and dissected at different levels by steep-walled valleys draining towards either north or south versants. According to isotopic studies, this upland sector, which concentrates many dolines, is considered the main recharge area for deep aquifers of Campo de Dalías aquifers (Vallejos et al., 1997). Dolines, relatively shallow, bowl-shaped depressions, are typical features in limestone terrains; however, little detailed work has been done on infiltration–runoff processes in their catenas. The landscape of dolines and slopes in this area is a mosaic of rock outcrops and patches of bare soil with rock fragment cover, which are interspersed with patches of vegetation. Currently, there are still important knowledge gaps on hydrological processes in this karst landscape: (1) how do surface characteristics and topography affect surface hydrology; (2) interaction of rock outcrops, fractured rocks, rock fragments, and vegetation, and their relative importance in controlling the hydrological response of soils in such karstic areas, and (3) how these factors interact to explain infiltration–runoff observed at different spatial scales. To address these knowledge gaps, we postulate that soil surface components (vegetation, rock outcrop and fragments, fracture, and soil crust), antecedent soil moisture, and rainfall characteristics play great roles in regulating infiltration–runoff processes in karst landscape, and that infiltration and/or runoff at the plot and slope scales could be predicted by different variables of soil surface and/or rainfall characteristics respectively. Therefore, we measured the partitioning of runoff–infiltration at two spatial scales: (1) micro-plot scale (0.24 m^2), using rainfall simulation experiments, and (2) hillslope scale, using water-level measurements monitored in an *aljibe* (a local underground cistern dug at the colluvium) draining a 9000-m^2 catchment (van Wesemael et al., 1998). This study would generate valuable information about how surface characteristics and landscape attributes contribute to explain the hydrological behaviour of Mediterranean carbonate karst ecosystem.

2. Material and methods

2.1. Study area

The study area was located in the Sierra de Gádor, a mountain range of up to 2242 m a.s.l. in southeastern Spain, just west of the city of Almería (Fig. 1). It consists of a thick series of Triassic carbonates, i.e., highly permeable and fractured limestones and dolomites underlain by intercalated calcschists of low permeability and by impermeable metapelites of Permian age at the base (Pulido-Bosch et al., 1993). A system of faults on the fringe of the coastal plain (Campo de Dalías) delimits the footslopes. The Sierra de Gádor has a Mediterranean climate characterised by dry hot summers, wet warm springs and autumns and wet cold winters. There are strong altitudinal gradients in annual precipitation and temperature. Mean annual precipitation is 260 mm in Alhama de Almeria (520 m.a.s.l.) and approximately 650 mm near the summit of the Sierra de Gador (2246 m.a.s.l.). Mean annual precipitation increases by about 23 mm for every 100 m increase in elevation. Mean annual temperatures are 9 °C near the summit and 18 °C at the foot of the range. The thermal gradient is about −0.4 °C/100 m (Contreras, 2006; Contreras et al., 2008).

Llano de los Juanes, a relatively flat area located in the Sierra de Gádor at 1600 m.a.s.l. was selected as the study site. It is characterised by the presence of dolines and fissured and fractured outcrops favouring rapid infiltration. This area represents the main recharge area of the Sierra de Gador according to previous stable isotopic analyses performed in the region (Vallejos et al., 1997; Vandenschrick et al., 2002; Contreras et al., 2008). A detailed description of the site is provided by Li et al. (2007, 2008) and Contreras et al. (2008). This area was severely deforested 100–150 years ago (Oyonarte et al., 1998), and at the present time, land is used for grazing sheep and goats. Mean annual precipitation measured in Llano de los Juanes from September 2003 to August 2010 was 525.8 mm. This value was very close to 537.5 mm y^{-1} estimated in the area based on rainfall data recorded in nearby meteorological stations (Contreras et al., 2008). Soils belonging to the Lithic Haploxeroll–Lithic Ruptic Argixeroll complex (Oyonarte, 1992), are very thin (generally <0.2 m) and rocky except at the bottom of some dolines where the depth can reach >0.5 m. All soil horizons are composed dominantly of silt (40–55%) and clay (26–52%). Organic matter content is relatively high at the surface, ranging from 1.6% to 11.9% (Table 1). Vegetation cover is generally 50–60% and consists mainly of patchy dwarf perennial shrubs (30–35%) and grasses (20–25%). The woody shrubs include *Genista pumila* (7–13%), *Thymus serpylloides* (4–17%) and *Hormathophylla spinosa* (2–6%). The herbaceous components are mostly *Festuca scariosa* (14–20%) and *Brachypodium retusum* (2–4%).

The landscape is a mosaic of rock outcrops, bare soils with a sparse rock fragment cover, and dispersed vegetation (plant tussocks and

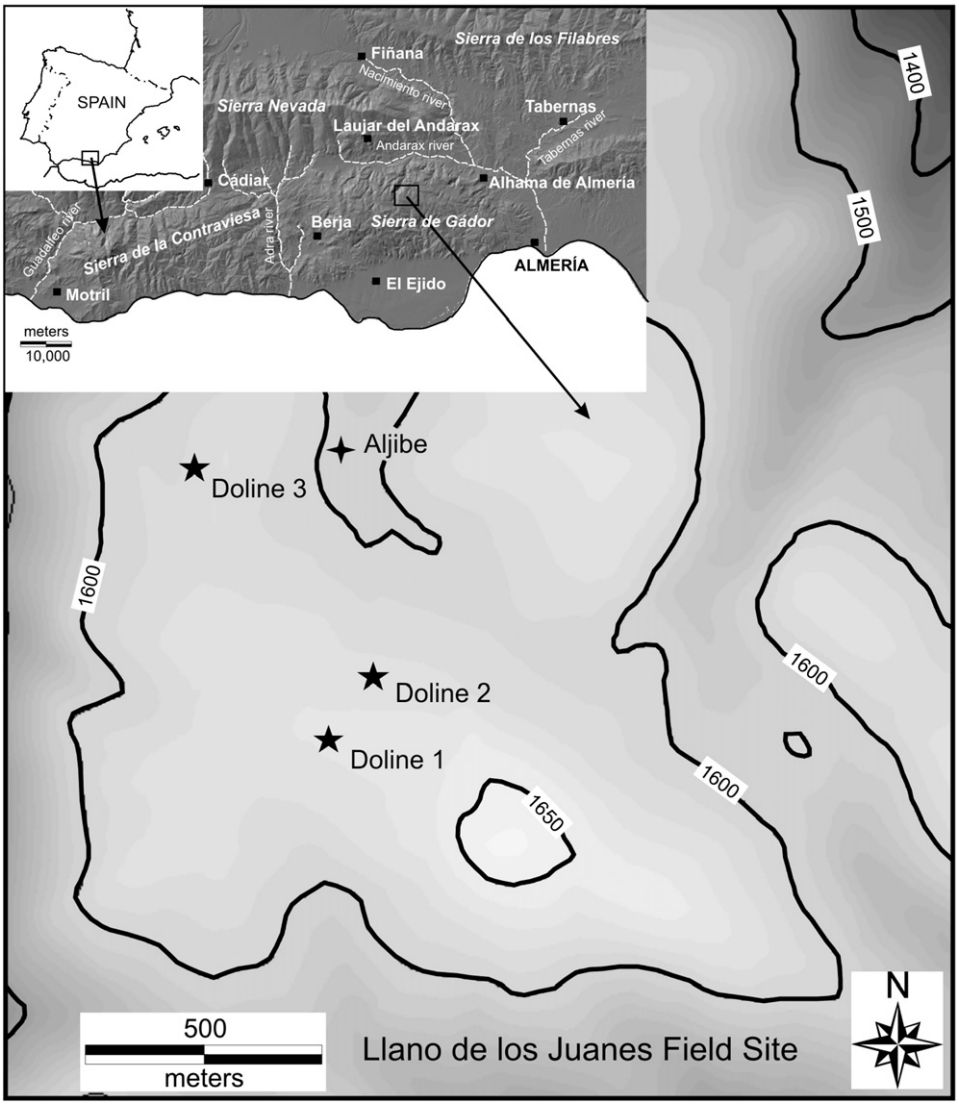

Fig. 1. Location and digital elevation model of the study area.

shrubs). Vegetation usually grows on fractured rocks. As previous field surveys have shown (Li et al., 2007, 2008), dolines in Llano de los Juanes are landscape entities where different soil surfaces and slope segments typical of the Sierra de Gádor are represented as short (20–50 m) catenas (Fig. 2A). Therefore, experimental sites were mainly selected in three dolines. Four topographical positions (top, upper, middle, and bottom) were selected in these three dolines, representing a convex, planar, and concave catena, respectively (Fig. 2A). A detailed description of these dolines has been reported by Li et al. (2007). In addition, two topographical positions were chosen at the upper and middle sections of a hillslope draining to an *aljibe* (underground cistern), which is a typical local water harvesting system that collects runoff water from hillslopes for watering livestock (Fig. 2B; van Wesemael et al., 1998). The hillslope is characterised by thin and rocky soil with a pattern of rock outcrops on the crest and shoulders and a colluvial mantle at the footslopes, where the *aljibe* has been constructed. Data about vegetation cover and rock fragments, organic matter content, soil texture and unsaturated hydraulic conductivity for the different topographical positions in the three dolines and hillslope with the *aljibe* are presented in Tables 1 and 2.

2.2. Simulated rainfall experiments at the micro-plot scale

To determine the effects of surface type and antecedent soil moisture on infiltration and runoff, seventy rainfall simulation experiments in total were conducted in 35 plots each under dry and wet conditions in the three dolines and one hillslope with the *aljibe*. Rainfall simulation experiments were performed on different types of soil surface, including bare soil, vegetated soil, rock fragment covered soil, and rock outcrops (Table 2). Percentages of cover in each plot were measured using photographs taken by a digital camera and analysed with the Optimas 5.2 image analysis system.

Rainfall simulations were carried out using an improved version of the sprinkler-type simulator developed by Cerdà et al. (1997). Such rainfall simulators, combined with runoff plots, have been widely used in the Mediterranean semiarid landscape for micro-plot studies of infiltration and runoff generation (e.g., Solé-Benet et al., 1997; Arnau-Rosalén et al., 2008; Mayor et al., 2009), although errors in the measurements may be caused by lateral seepage of water beneath and beyond the boundaries of the edges of rings (Duley and Domingo, 1943; Joel et al., 2002). Rainfall was supplied by a 2-m high nozzle onto a 1-m^2 target area. Runoff was collected from a 0.24-m^2 circular

Table 1
Particle size distribution, organic matter content and unsaturated hydraulic conductivity at different tensions of surface soils in different topographic positions in the three dolines and the *aljibe* hillslope.

Landscape position	Organic matter (%)	Particle size composition USDA (%)			Unsaturated hydraulic ($mm\ h^{-1}$) conductivity. at different tensions		
		Sand	Silt	Clay	3 cm	6 cm	12 cm
Doline 1							
Bottom	4.95	14.21	50.46	35.33	7.35	2.97	0.81
Middle	6.76	16.33	49.08	34.59	11.32	5.73	2.02
Upper	8.06	12.37	51.26	36.37	6.01	3.39	1.76
Top	4.37	13.14	52.54	34.32	26.60	9.66	2.53
Doline 2							
Bottom	3.35	4.43	44.38	51.19	3.96	1.40	0.65
Middle	7.15	21.91	49.57	28.52	25.64	4.46	1.43
Upper	6.88	14.68	55.19	30.13	28.27	11.79	2.84
Top	7.63	6.67	41.15	52.18	33.84	11.74	2.81
Doline 3							
Bottom	1.66	16.39	40.53	43.08	4.49	2.21	0.89
Middle	11.97	15.45	57.93	26.62	10.32	3.80	0.63
Upper	11.13	14.26	53.70	32.04	65.85	14.65	2.53
Top	6.45	16.69	45.83	37.48	39.77	11.85	2.49
Aljibe slope							
Bottom	5.23	12.06	32.51	55.43	3.77	1.04	0.36
Middle	8.71	9.06	43.22	47.72	19.96	1.93	0.38
Upper	9.44	19.88	58.75	21.37	69.72	2.37	0.34

plot within the target area bounded by a 0.55-m-diameter metal ring and recorded by an automated tipping-bucket gauge. The size of the plot was chosen in order to measure infiltration on representative soil surface types while minimising the impact of topography (Cantón et al., 2002). The average (±SD) simulation rainfall intensity was $53.2 \pm 11.0\ mm\ h^{-1}$, which is not significantly different from the maximum hourly rainfall intensity estimated in the area for a 10-year return period ($50\ mm\ h^{-1}$) (Elías-Castillo and Ruiz-Beltrán, 1979). During rainfall simulations, the volumetric water content on dry and wet soil conditions ranged from 1.5 to 8.3% and 22.0 to 37.4%, respectively. Rainfall simulations for the first run lasted up to 60 min if no steady runoff (no variations in runoff rate during 5 min) was obtained earlier. In order to know how much rainfall would be needed to generate runoff in vegetated plots, a continuous simulated rainfall (up to 4.8 h) was applied on plot 3 with 95% of *F. scariosa* until the steady runoff condition was reached. A 15 minute time lapse was given between the first (dry) and the second (wet) runs. The duration of the wet run ranged from 14 to 23 min. Following Solé-Benet et al. (1997), time to ponding, time to crack closure, and time to runoff were recorded for each rainfall simulation. Wetting depths (maximum vertical water penetration depth) and water flow path in the soil profile were recorded at the end of the second run by excavating the soil and photographing with a digital camera. Surface soil samples (0–5 cm) for determining moisture content were taken before and after each experiment. Runoff coefficient was calculated as the ratio of the total runoff and the total applied rainfall. Infiltration rates were calculated by subtracting runoff rates from rainfall intensity. The steady infiltration rate was estimated by fitting the infiltration rates to an exponential decay function based on the Horton equation (Horton, 1940). The Hortonian equation was chosen, as in the Mediterranean landscape the dominant mechanism of runoff generation at plot and

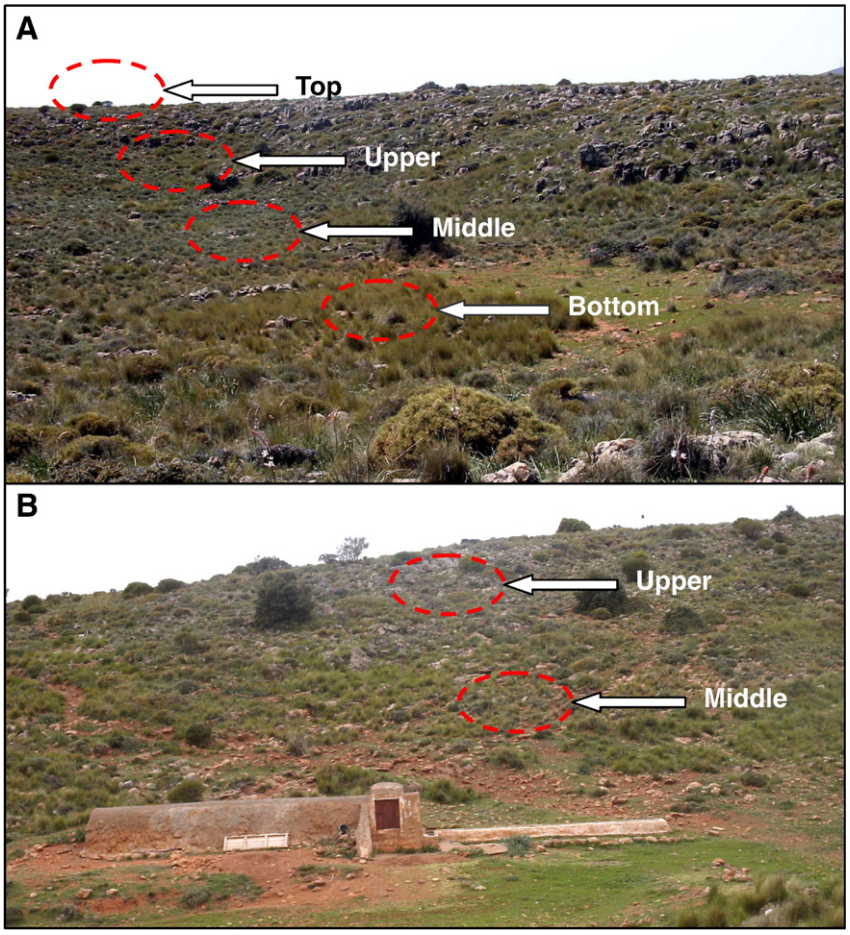

Fig. 2. Landscape of (A) a planar doline (doline 2) and (B) the *aljibe* slope, showing the different topographic positions used in this study. This particular *aljibe* is a concrete-roofed cistern located at the bottom of the hillslope which collects the runoff generated from a small catchment of 9000 m^2.

Table 2
Characteristics of 35 plots in which rainfall simulations were performed (V = vegetation coverage; R_f = rock fragment coverage; B_s = bare soil coverage; and R_o = rock outcrop coverage). Litter was included in V and its predominance is expressed in the 'vegetation type' column when its coverage was higher than the plant coverage.

Plot #	Location	Landscape position	Aspect (°)	Slope (°)	Vegetation type	V (%)	R_f (%)	B_s (%)	R_o (%)
1	Doline 1	Bottom	273	0.0	*T. serpylloides*	35.7	5.0	59.3	0.0
2	Doline 1	Bottom	75	6.3	*F. scariosa*	8.0	85.8	6.2	0.0
3	Doline 1	Middle	70	14.4	*F. scariosa*	96.0	2.0	2.0	0.0
4	Doline 1	Bottom	355	0.0	*F. scariosa*	3.0	2.0	95.0	0.0
5	Doline 1	Bottom	155	0.0	*F. scariosa*	2.0	96.0	2.0	0.0
6	Doline 1	Bottom	165	0.0	*H. spinosa*	98.0	0.0	2.0	0.0
7	Doline 1	Middle	72	9.9	*G. pumila*	100.0	0.0	0.0	0.0
8	Doline 1	Upper	105	18.9	Litter	5.0	90.0	5.0	0.0
9	Doline 1	Upper	105	43.2	*H. spinosa*	52.8	2.0	14.9	25.3
10	Doline 1	Top	61	14.4		0.0	0.0	0.0	100.0
11	Doline 1	Top	310	0.0	Litter	2.0	10.0	88.0	0.0
12	Doline 1	Top	310	0.0	Litter	2.0	93.0	5.0	0.0
13	Doline 1	Top	310	26.1	*F. scariosa*	89.4	4.6	5.0	0.0
14	Doline 2	Bottom	15	0.0	Litter	84.1	10.9	5.0	0.0
15	Doline 2	Bottom	195	0.0	Litter	2.0	2.0	96.0	0.0
16	Doline 2	Bottom	110	0.0	*F. scariosa*	81.5	0.0	8.5	0.0
17	Doline 2	Upper	116	22.5	*T. serpylloides*	82.5	12.5	5.0	0.0
18	Doline 2	Upper	127	29.7	Litter	2.0	96.0	2.0	0.0
19	Doline 2	Top	105	27.0	*T. serpylloides*	12.5	29.5	2.0	56.0
20	Doline 2	Top	235	0.0	Litter	5.0	22.3	72.7	0.0
21	Doline 3	Bottom	330	0.0		0.0	56.0	44.0	0.0
22	Doline 3	Middle	10	8.1	*F. scariosa*	7.0	10.0	83.0	0.0
23	Doline 3	Middle	45	36.9	*T. serpylloides*	56.8	5.0	18.0	20.2
24	Doline 3	Middle	48	21.6	*F. scariosa*	95.0	0.0	5.0	0.0
25	Doline 3	Upper	6	22.5	*T. serpylloides*	11.0	83.0	8.0	0.0
26	Doline 3	Upper	10	40.5	*G. pumila*	93.0	2.0	5.0	0.0
27	Doline 3	Top	25	18.0	*T. serpylloides*	7.0	2.0	7.0	84.0
28	Doline 3	Top	357	0.0	*F. scariosa*	10.0	85.0	5.0	0.0
29	Doline 3	Top	355	0.0	*G. pumila*	90.0	8.0	2.0	0.0
30	Hillslope	Upper	295	44.1		0.0	5.0	95.0	0.0
31	Hillslope	Upper	295	50.4	*F. scariosa*	32.0	5.0	8.3	54.7
32	Hillslope	Upper	290	48.6	*F. scariosa*	98.0	0.0	2.0	0.0
33	Hillslope	Middle	290	18.0	*F. scariosa*	27.7	30.0	42.3	0.0
34	Hillslope	Middle	295	24.3	Litter	2.0	4.2	93.8	0.0
35	Hillslope	Middle	282	17.1	Litter	1.0	2.0	97.0	0.0

hillslope scale is the infiltration excess or Hortonian overland flow (Yair and Lavee, 1985; Lavee et al., 1998; Beven, 2002), although with strong spatial discontinuity (Calvo-Cases et al., 2003). The Horton model has been widely used for steady infiltration estimation (e.g., Lavee et al., 1991; Solé-Benet et al., 1997; Imeson et al., 1998; Calvo-Cases et al., 2003; Arnau-Rosalén et al., 2008; Mayor et al., 2009) in similar environments.

2.3. Monitoring runoff response at hillslope scale

Runoff response in an *aljibe* draining a 9000-m^2 catchment (Fig. 2B) was studied under natural rainfall conditions from September 1, 2003 to March 15, 2005. A water level pressure sensor (model WL14, Global Water Inc., USA) with an accuracy of 5 mm was installed in the *aljibe* to monitor runoff water. Data was continuously recorded and the 30-min average was saved in a datalogger. A standard rainfall gauge was also installed at the top of the hillslope to measure the amount and intensity of precipitation. Rainfall events were discretized by assuming a time without rainfall between events of 6 h. The drainage area of the *aljibe* was estimated based on a 0.5-m-resolution aerial photograph (Junta de Andalucía, 2005) and field survey. Runoff coefficients were estimated for each rainfall event taking this drainage area into account. As evapotranspiration was also measured in the area for other purposes during the entire study period (Cantón et al., 2010), assessment of hillslope-scale infiltration was quite good. Because of the lack of soil moisture measurements, the effect of antecedent soil moisture on runoff generation at hillslope scale was evaluated using the accumulative precipitation in the previous 20 days prior to each rainfall event (AP_{20}) as a surrogate of the antecedent soil wetness condition.

2.4. Data analysis

Data from each rainfall simulation were analysed by surface type (bare soil, vegetated soil, and rock fragment covered surfaces). Stepwise linear regression analyses were used to find the best empirical relationships for predicting constant infiltration rate and runoff coefficient at both micro-plots and hillslope using the rainfall characteristics during the simulations (intensity and volume of water supplied), the soil surface variables (vegetation, litter, bare soil, rock fragments, and rock outcrop) and antecedent soil water content or AP_{20}. All statistical procedures were completed using Statistica 6.0 (StatSoft Inc., 2001).

3. Results

3.1. Runoff-infiltration from micro-plot rainfall simulations

3.1.1. Influence of soil surface types

Rainfall simulation results are presented in Table 3. None of the vegetated plots (n = 12) with a plant cover higher than 50% (Fig. 3) had runoff after one hour of rainfall. In plot 3, intermittent runoff occurred after 4.8 h of simulated rainfall, showing that about 260 mm of rainfall was necessary to generate runoff under initially dry soil conditions with a constant rainfall intensity of 54 mm h^{-1}. However, only 12 mm of rainfall was required to generate runoff when the second run of rainfall simulation was performed under wet soil conditions.

In rock outcrop plots (n = 4), runoff coefficients were high (59.0–79.5%) when no cracks were present in the surface (plot 10), and the rainfall required to initiate runoff was less than 3 mm under dry conditions (Fig. 4). However, when cracks were present (plot 27),

Table 3
Parameters obtained from runoff-producing plots where rainfall simulations were performed: P = total rainfall applied, T_p = time to ponding, T_r = time to runoff, R_c = runoff coefficient, R_r = average runoff rate, FR_r = final runoff rate, FI_r = final infiltration rate; R_{nr} = rainfall necessary to initiate runoff, and SW = surface volumetric soil water content.

Surface type	Plot number	Surface wetness	P (mm)	T_p (min.)	T_r (min.)	R_c (%)	R_r (mm/h)	FR_r (mm/h)	FI_r (mm/h)	R_{nr} (mm)	SW (%)
Vegetated soil	1	Dry	23.6	9.7	19.4	4.0	5.8	5.43	42.89	15.6	3.82
		Wet	13.3	1.9	1.0	14.7	7.7	8.92	39.40	1.0	30.00
	3	Dry	269.9	n.a.	288.7	0.1	1.3	0.30	53.67	259.7	n.a.
		Wet	13.5	n.a.	12.4	0.7	1.9	0.38	53.59	11.2	n.a.
Rock fragment covered soil	2	Dry	27.9	2.3	14.7	5.5	5.6	5.75	48.22	13.2	5.67
		Wet	18.7	1.2	1.5	12.2	6.6	8.64	45.51	1.4	29.94
	5	Dry	79.1	9.6	48.9	0.2	0.8	0.89	78.06	64.4	5.72
		Wet	20.3	1.2	13.2	0.7	4.4	3.92	75.03	17.3	27.76
	12	Dry	35.2	57.0	n.r.	n.r.	n.r.	n.a.	n.a.	n.r.	2.75
		Wet	8.8	4.7	13.9	4.3	15.7	5.94	29.22	8.1	29.22
	21	Dry	38.8	3.4	9.2	41.9	44.4	63.32	11.31	11.5	4.09
		Wet	19.9	0.3	0.7	67.6	52.7	62.43	12.20	0.8	37.31
Bare soil	4	Dry	44.5	2.6	14.5	19.1	26.4	37.44	41.51	19.0	5.46
		Wet	22.7	0.6	1.5	20.9	18.1	19.76	59.19	2.0	26.72
	11	Dry	29.1	4.1	21.3	18.2	14.7	17.50	23.21	14.4	2.59
		Wet	14.1	0.7	2.9	24.8	11.7	14.23	26.48	2.0	26.19
	20	Dry	52.1	26.8	57.0	5.4	n.a.	0.05	54.84	52.1	3.08
		Wet	18.5	3.4	14.4	3.5	6.7	6.84	48.05	13.2	27.16
	22	Dry	53.2	29.0	n.r.	n.r.	n.r.	n.a.	n.a.	n.r.	5.45
		Wet	19.4	2.4	13.0	8.4	11.0	36.68	14.52	11.5	35.15
	33	Dry	39.9	n.a.	17.8	3.1	3.3	5.08	54.74	17.8	2.86
		Wet	14.6	n.a.	6.4	2.0	2.2	3.29	56.53	6.4	34.28
	34	Dry	45.7	39.2	34.1	6.6	7.0	12.19	33.30	25.9	2.28
		Wet	12.0	2.1	2.2	65.4	34.6	42.22	3.27	1.7	30.95
	35	Dry	27.0	8.4	9.7	20.6	16.4	23.72	30.25	8.7	1.55
		Wet	13.5	0.7	1.2	45.8	26.8	28.70	25.27	1.0	32.32
Rock outcrop	10	Dry	12.1	0.9	2.5	59.0	27.6	12.79	28.84	2.8	n.a.
		Wet	9.0	0.5	1.0	79.5	33.4	14.45	27.18	0.6	n.a.
	27	Dry	40.7	0.6	15.3	10.4	10.3	16.02	45.04	15.6	5.03
		Wet	15.5	0.3	0.9	28.5	18.5	23.61	37.45	0.9	33.79

n.a. = not available.
n.r. = no runoff.

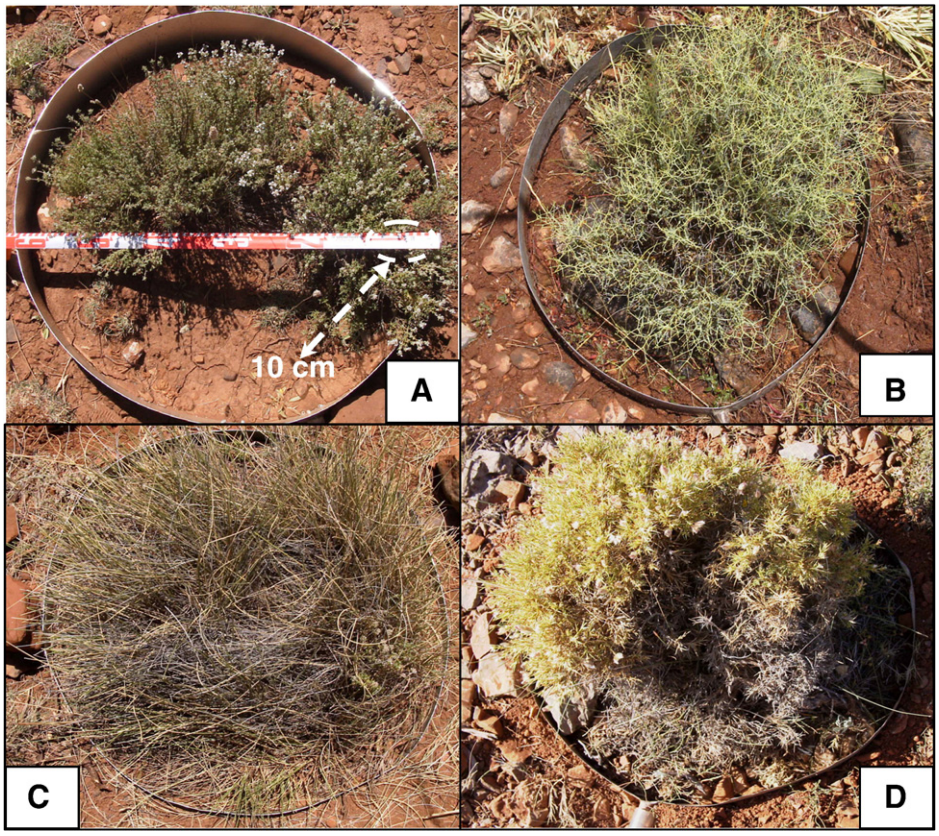

Fig. 3. Plant-covered plots (55 cm in diameter) contained four types of vegetation: (A) = *Thymus serpylloides* (plot 1), (B) = *Hormathophylla spinosa* (plot 9), (C) = *Festuca scariosa* (plot 24), (D) = *Genista pumila* (plot 29).

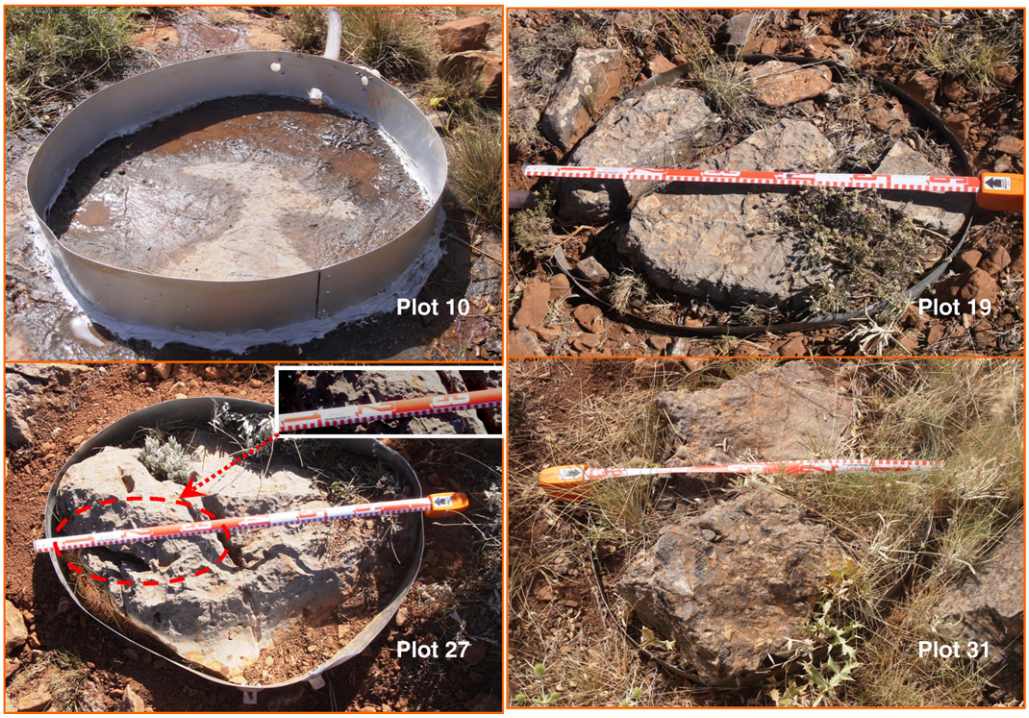

Fig. 4. Illustrations of plots with rock outcrops: Plots 10 without cracks; plot 27 with small crack in the rock, plots 19 and 31 with deep cracks in the rock and vegetation.

runoff coefficients were drastically reduced to 10.4% and 28.5% when simulations were run under dry and wet soil conditions, respectively. In addition to these differences in runoff coefficients, generation of runoff under wet soil conditions in plots 10 and 27 occurs relatively fast, as <1 mm of rainfall was needed to initiate runoff. No runoff was observed in plots 19 and 31 because these had a lower rock cover (~55%), vegetation and more cracks than plots 10 and 27 (Fig. 4).

In plots with rock fragment cover of more than 50%, the position and size of the rock fragments were the main controls of the runoff response ($n=8$). Relatively large runoff coefficients were found at the bottom of the dolines (e.g., plots 2 and 21) where rock fragments are usually embedded in a surface seal which inhibits infiltration. However, no runoff was observed on doline slopes (plots 8, 18, 25 and 28) where rock fragments rested on the soil surface preventing surface sealing. Only in plot 12, located at the top of doline 1, runoff (4.3% of simulated rainfall) was produced when the rainfall simulation was performed under wet soil conditions. The time required to initiate runoff was on average twice as long in the plot located at the upper positions of the slopes (e.g., plot 12) than in the ones at the bottom sections of the dolines (e.g., plot 21) or the hillslope with the *aljibe* where rock fragments were partly buried in a surface seal (Table 3). Under such conditions, there was a strong negative relationship between the rock fragment cover (*RF*) and the runoff coefficient: $Rc = -1.704 \times RF + 162.1$ ($R^2 = 0.99$, $p<0.01$, $n=4$).

All plots with bare soil cover higher than 50% ($n=10$) produced runoff, except plot 22, at the middle slope of doline 3, during the dry run of the simulated rain, and plot 30, at the upper part of *aljibe* slope, during both the dry and wet runs of rainfall simulation. Runoff coefficients ranged from 3.1% to 20.6% on dry soil surfaces, and from 2.0% to 65.4% on wet soil surfaces. In bare plots with runoff, the rainfall amount needed to initiate runoff ranged from 8.7 to 52.1 mm on dry soils and from 1.0 to 13.2 mm on wet soils. The average wetting depth in all bare plots was 15 cm, i.e. half of the observed value for vegetated soils and rock outcrops and, 2/3 less than the value measured in plots with rock fragment cover. However, it should be noted that when the effect of soil crusting was analysed separately, the average wetting depth measured in the non-crusted soils (e.g., plots 22, 30) was nearly 4 times deeper than in crusted soil surfaces (e.g., plots 4, 15) suggesting that soil crusting has a positive impact on the runoff generation.

Vegetated plots had the highest average steady infiltration rate (Fc) of 52.79 ± 2.94 mm h^{-1}, followed by surface types dominated by rock fragments (49.99 ± 4.28 mm h^{-1}), rock outcrops with cracks (41.28 ± 1.53 mm h^{-1}), mixtures (MIX) of vegetation, rock fragments and bare soil (37.34 ± 8.40 mm h^{-1}), bare soil (33.70 ± 9.17 mm h^{-1}) and rock outcrops (29 mm h^{-1}) without cracks (Fig. 5).

3.1.2. Influence of antecedent soil moisture

Soil moisture content at the beginning of the rainfall simulations had a substantial impact on runoff–infiltration processes (Table 3). Antecedent volumetric soil moisture values ranged from 1.6–5.7% for dry soil surfaces to 26–37% for wet ones (Table 3). For plots with runoff, time and rainfall to runoff were on average four times higher when rainfall simulations were performed under dry soil moisture conditions. As can be expected, runoff coefficients and rates increased on average during the second run when the soil was wetter. Runoff coefficients ranged from 0.1% to 59.0% for the first runs and from 0.7%

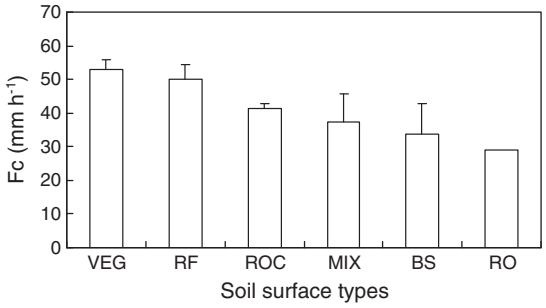

Fig. 5. Comparison of steady infiltration rate (Fc) (mean + one standard error) for different surface types with >80% coverage dominated by vegetation and litter (VEG) ($n=11$), rock fragments (RF) ($n=4$), rock outcrops with cracks (ROC) ($n=3$), bare soil (BS) ($n=4$), and rock outcrops (RO) ($n=1$). MIX ($n=4$) represents mixture of vegetation, rock fragments, and bare soil with each coverage less than 50%.

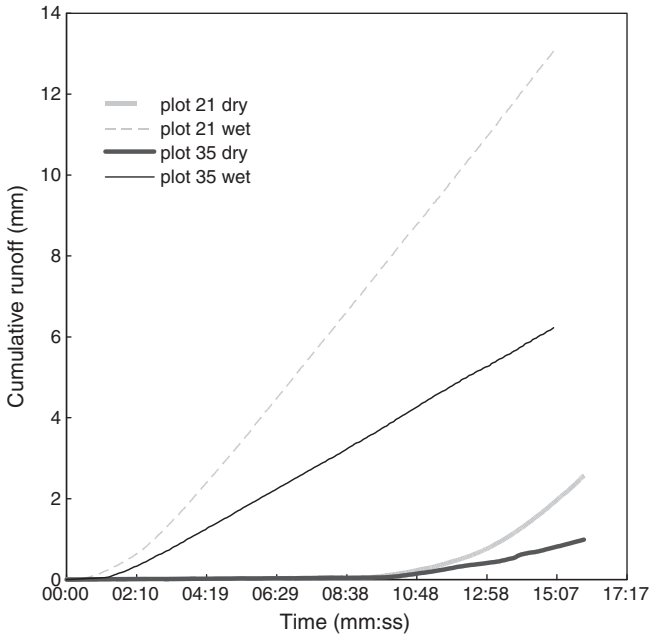

Fig. 6. Cumulative runoff versus time during dry and wet runs of rainfall simulations for plot 21 and plot 35. Runoff increases sharply with time during the wet runs as compared to the dry runs.

to 79.5% during the second ones while runoff rates ranged from 0.8 to 44.4 mm h^{-1} for dry soil conditions and from 1.9 to 52.7 mm h^{-1} for wet soil conditions (Table 3). Fig. 6 clearly shows how runoff increases sharply with time during the wet runs as compared to dry runs suggesting that infiltration rates are high during the first stages of the rainfall event when the soil is dry. Sometimes, this initial stage may even last several hours due to macropore flow resulting from root channels, rock cracks and fissures or cracks in clay.

When hydrological variables and antecedent soil moisture content were analysed as a whole, the time and the rainfall needed to initiate runoff were significantly ($p<0.01$, $n=24$) and negatively correlated with antecedent soil moisture ($r=-0.63$ and $r=-0.58$, respectively). However, the impact of antecedent soil moisture on runoff coefficients and rates was not clear and no significant relationships ($p>0.1$, $n=24$) were found for either variable ($r=0.34$ and $r=0.26$, respectively) probably because of the effects that the other variables had on the runoff generation. Also no significant relationship was found between soil moisture content and the Fc ($p>0.1$, $n=18$).

3.1.3. Relationships between infiltration–runoff and other variables

Linear regression equations were obtained for predicting runoff coefficients (*Rc*) and steady-state infiltration rates (Fc) from rainfall characteristics, soil surface variables (land cover type coverage) and antecedent soil water content. The best linear model for estimating the runoff coefficient (%) in the micro-plots was:

$$Rc = -13.26 + 0.12\,BS + 0.33\,I - 0.07\,VEG, \quad \left(R^2 = 0.41, p<0.01, n = 63\right) \tag{1}$$

where *BS* is bare soil coverage (%), *I* is simulated rainfall intensity (mm h^{-1}), and *VEG* is the vegetation cover (%).

Vegetation and litter cover and rainfall intensity were the main predictors of the steady infiltration rate:

$$Fc = 3.21 + 0.64\,VEG + 0.45\,I + 1.72\,L, \quad \left(R^2 = 0.41, p<0.05, n = 18\right) \tag{2}$$

where Fc is the steady-state infiltration rate (mm h^{-1}), *VEG* and *L* are vegetation and litter cover (%), respectively, and *I* is the simulated rainfall intensity (mm h^{-1}).

3.2. Runoff on the hillslope with the aljibe

Annual precipitation between September 2003 and August 2004 was 506.7 mm, somewhat lower than the average for the study area. However, the 2004–2005 hydrological year was very dry with only 212.1 mm of rainfall (Fig. 7). Total precipitation recorded during the

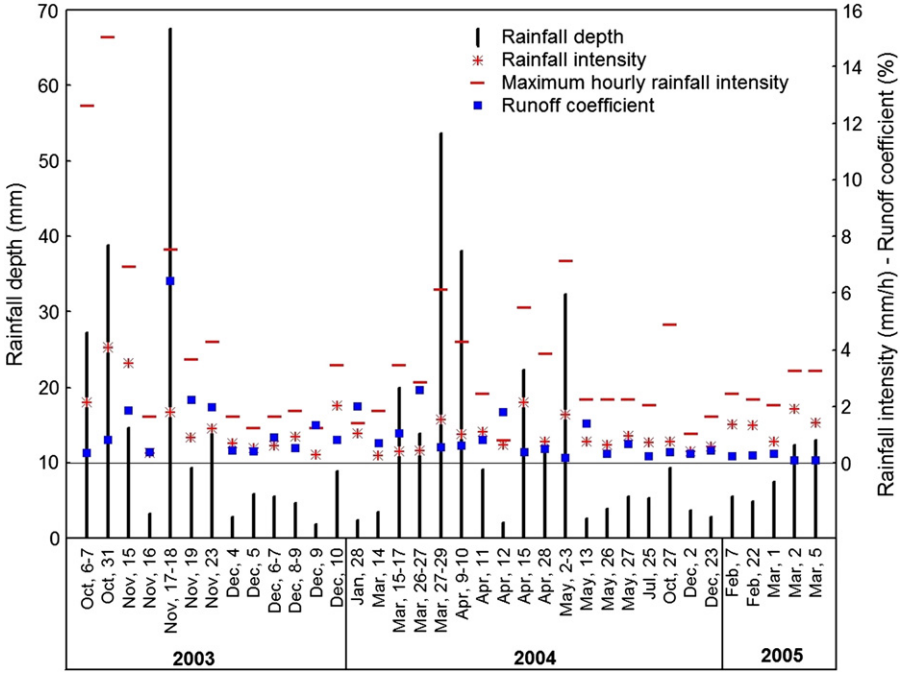

Fig. 7. Distribution of rainfall events and their main characteristics (depth, average intensity and maximum hourly intensity) and event-based runoff coefficients (%) from 1 Sept 2003 until 15 March 2005 in the *aljibe* hillslope.

study period (September 1, 2003 to March 15, 2005) was 705.4 mm, which was distributed over 76 rainfall events with amount over 1 mm, 36 of which induced a response in the water level in the *aljibe* (Fig. 7). Average runoff coefficients were 1.44% in the 2003–2004 year and less than 0.1% from 1 September 2004 to 15 March 2005. All the rainfall events with runoff occurred during the wet season, from October to May. Maximum hourly rainfall intensities (I_{60}) for those events ranged from 0.81 mm h^{-1} to 15.05 mm h^{-1}, i.e. about 68 and 3.5 times less than the intensity of the rainfall simulations. Of the 36 runoff events, only one had a runoff coefficient over 5%, and in 47% of the cases, the runoff coefficient was less than 0.5% (Fig. 7). The highest runoff and rainfall event occurred on November 17–18, 2003 (Fig. 8). The total rainfall recorded on these two days was 67.5 mm, with an average intensity of 1.81 mm h^{-1} with a peak intensity of 14.64 mm h^{-1} in 5 min after the rain started (Fig. 8). According to the total rainfall, the return period for this event in the study area was 2.5 years (Elías-Castillo and Ruiz-Beltrán, 1979). The maximum hourly rainfall intensity (I_{60}) throughout the event was 7.53 mm h^{-1}, i.e. seven times lower than the rainfall intensity used for rainfall simulations. A total volume of 39.38 m^3 was collected in the *aljibe* in 37.41 h, which means an overall runoff coefficient of 6.41%. The maximum volume of runoff recorded in 30 min. was 6.25 m^3 for a rainfall of 2.85 mm, i.e. a peak runoff coefficient equal to 24% in 30 min., and it took place after 26.5 h from the start of the rainfall. Assuming that evapotranspiration was negligible during the rainfall event, the average infiltration rate for the whole event was 1.69 mm h^{-1} (i.e., 63.17 mm in 37.41 h) with an instantaneous peak of 13.9 mm h^{-1}. Total infiltration at the end of the event was 93.59% of the rainfall.

On the hillslope, overall runoff was quite low, i.e., 7.4 mm, during the 18-month monitoring period. According to the rain that fell during the period (705.4 mm) and the actual evapotranspiration measured using the eddy covariance technique (406.0 mm), we conclude that infiltration in the slope with the *aljibe* reached 292.0 mm, i.e. ~41% of the total rainfall. This value agrees with the mean annual value, i.e. 36–38%, estimated by Contreras et al. (2008) for the same catchment using a regional satellite-based ecohydrological model. The value is also similar to the ones reported in the literature review of Calvo-Cases et al. (2003) for soils developed on highly-cemented calcareous rocks (dolomites and limestones).

In a similar way as we proceeded in micro-plots, multiple linear regressions yielded the following empirical equations for predicting the runoff in the slope:

$$Rd = 0.93P - 0.36I_{60} \quad \left(R^2 = 0.52,\ p<0.01,\ n = 36\right) \tag{3}$$

$$Rc = 0.039P + 0.007AP_{20} \quad \left(R^2 = 0.52,\ p<0.01,\ n = 36\right) \tag{4}$$

where Rd is runoff depth (mm), Rc is runoff coefficient (%), AP_{20} is the antecedent precipitation accumulated over 20 days prior to each rainfall event, P is the rainfall depth (mm) and I_{60} is the maximum hourly rainfall intensity (mm h^{-1}).

4. Discussion

4.1. Factors and interactions controlling micro-plot infiltration–runoff processes

The results of rainfall simulations confirm that soil surface characteristics (vegetation, fractures, and rock outcrops and fragments) play a dominant role in controlling runoff and infiltration at plot scale in the karst landscapes. Vegetation patches exert a clear and negative effect on runoff generation while bare patches and rock outcrops act as sources of runoff. This study particularly revealed and emphasised the importance of vegetation and the presence of rock fractures on the infiltration in the limestone karst landscape. The threshold of 260 mm required to generate runoff in plot 3 with 95% of *F. scariosa*, indicated that the infiltration rate was very high, suggesting that, at least at the micro-plot scale, vegetation patches probably act as sinks for almost all rainfall events in the area. Such a 260 mm rainfall event is well above the rainfall of 100–125 mm day^{-1} reported in the area by Elías-Castillo and Ruiz-Beltrán (1979) for a return period of 250 years and the 155 ± 14 mm day^{-1} that Martin Rosales (2002) estimated for a return period of 100 years in a nearby location (La

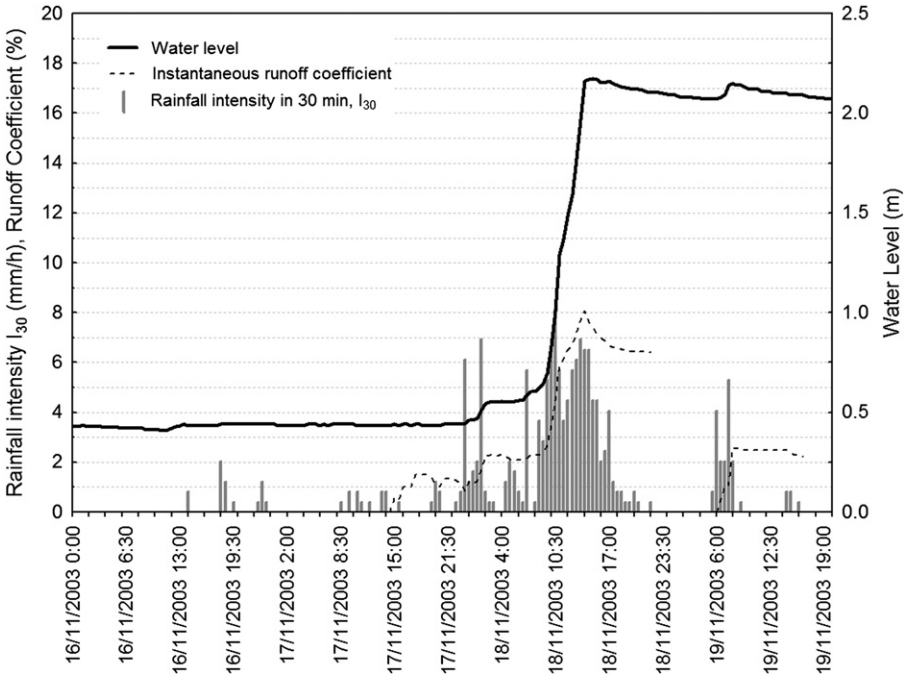

Fig. 8. Precipitation and runoff during the event of 17th–18th November 2003. Total precipitation was 67.5 mm, while total runoff in the *aljibe* hillslope was only 4.33 mm.

Zarba). Similarly, Calvo-Cases et al. (2005) also reported that soils covered by vegetation on limestone slopes became saturated and began to contribute to runoff during events of around 100 mm. The impact of vegetation in explaining high infiltration rates observed in micro-plots might be attributed to direct and indirect effects (Wilcox et al., 1988; Puigdefábregas, 2005) through: (1) its role in dissipating the kinetic energy of raindrops and hence avoiding surface sealing; (2) supply of organic matter and the improvement of soil structure and soil infiltration rate; (3) generation of macropores and channels associated with root and soil crack development. Fig. 9 shows that in plot 1, where the ground surface was characterised by the presence of bare soil and vegetation, the wetting front depth observed in the root area under the plant *T. serpylloides* was 6 cm deeper than that in the adjacent bare soil. These findings are consistent with our previous results which showed significantly greater hydraulic conductivity ($K(h)$) values at tension of 3 and 6 cm in vegetated surfaces than in bare soil surfaces (Li et al., 2008). The negative impacts of vegetation on runoff generation and its positive impacts on infiltration have also been highlighted in other semi-arid environments by other researchers. Quinton et al. (1997) described a negative relationship between runoff coefficient and vegetation cover ($R^2 = 0.36$, $p < 0.01$) in SE of Spain, and Wilcox (2002) reported that the presence of juniper trees promotes the infiltration of water into the soil surface and its rapid movement through the root zone as preferential flow in karst regions of Texas. Newman et al. (1998, 2004) documented that lateral subsurface flow in semiarid forests of ponderosa pine in New Mexico occurred mainly through root macropores and Bergkamp (1998) and Li et al. (2009) noted that rapid infiltration near vegetation clusters was related to preferential flow of water.

The effect of rock fractures promoting infiltration and reducing runoff was mainly attributed to the fact that cracks were primary pathways for preferential flow. Vegetation usually grows on fractured limestone rocks in a karst landscape. Rock cracks may be important conduits to transport runoff to the root zone or non-saturated zone and may serve as important rooting media for the plant growth if they are able to hold the infiltration water (Jones and Graham, 1993). The ambivalent effect of rock fragment cover on both infiltration rate and overland flow generation depends on various factors, such as position, size and cover of rock fragments as well as structure of the fine earth, as first described by Poesen and Ingelmo-Sanchez (1992). Infiltration is higher when rock fragments are on the soil surface (e.g. plots 8, 25, 28) as they generally prevent the soil from sealing. However, when

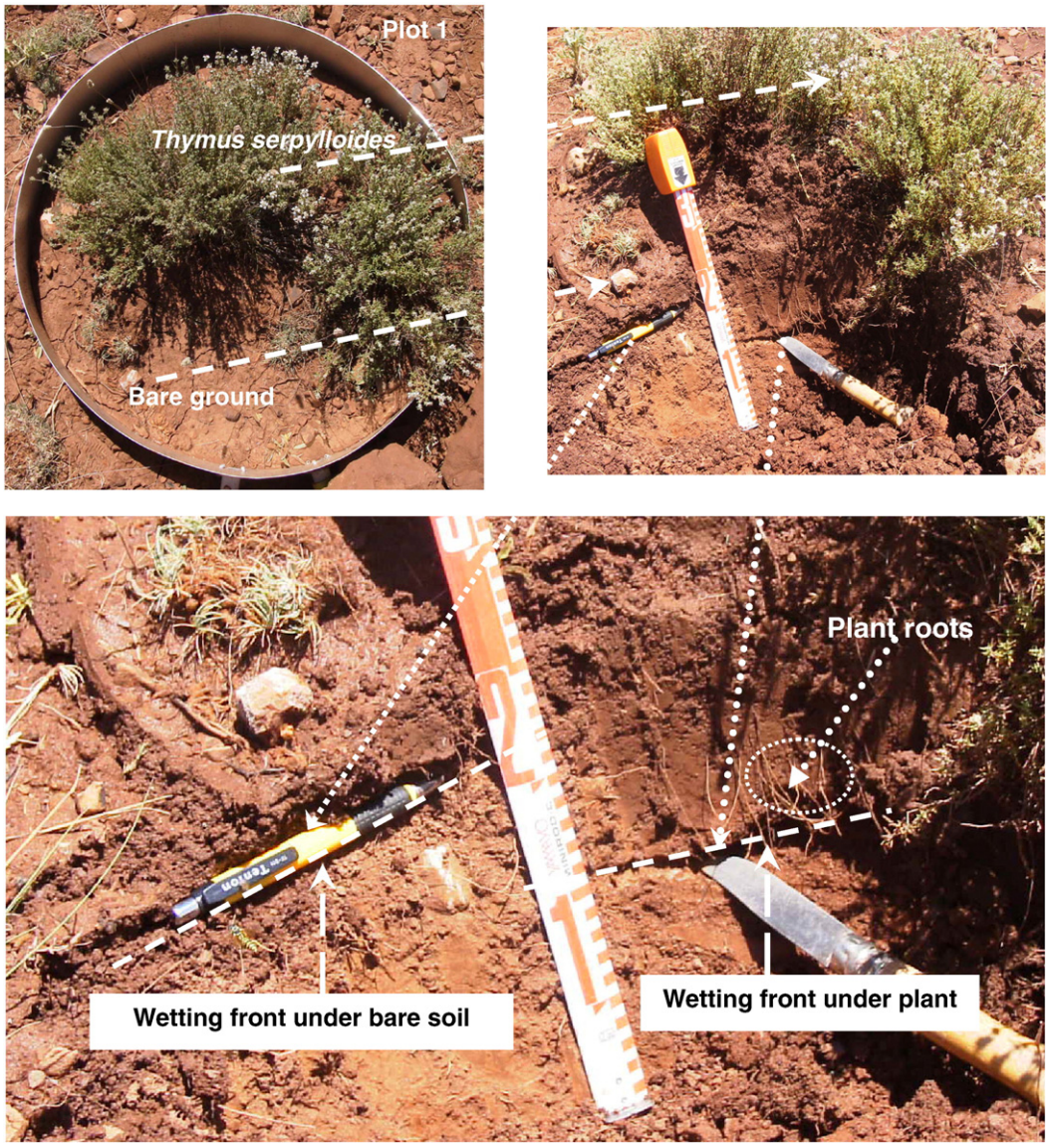

Fig. 9. Illustrations of observed wetting front under plant and adjacent bare soil after one hour of 55 mm simulated rainfall for plot 1 with plant of *Thymus serpylloides*.

rock fragments are embedded in the surface (e.g. plots 2, 5, 21), they contribute to the establishment of a continuous crust which inhibits infiltration and promotes runoff.

Our results from the micro-plot experiments strongly support previous findings on the strong spatial variability in the infiltration and runoff processes in semiarid limestone landscapes, and the complexity of these processes due to the role of diverse controlling variables and the interactions between them (Wilcox et al., 2007; Mayor et al., 2009). The presence of vegetation, dissolution cracks and fissures on rock outcrops, and soil crust on bare soil, as well as the ambivalent effect of rock fragments on runoff generation, adds more complexity to the spatial source-sink mosaic typical of karst landscapes. Spatial variability of the hydrological function was also strongly influenced by the topographic position and the antecedent soil moisture condition. All these interacting factors are a challenge for modelling non-uniform infiltration–runoff processes. The regression Eqs. (1) and (2) indicate that infiltration and runoff in the micro-plots is mainly controlled by the bare soil and vegetation cover as well as rainfall intensity. This has also been explicitly recognised by Bowyer-Bower (1993), and by Vahabi and Mahdian (2008). The latter have obtained similar equations explaining runoff generation at micro-plots in the Taleghan watershed (Iran) concluding that vegetation cover was the most influential factor in explaining runoff generation.

4.2. Responses of infiltration–runoff on the hillslope

On the slope with the *aljibe*, overall runoff (mostly below 1%) was quite low during the 18-month measuring period, and infiltration accounted for ~41% of the total rainfall amount, indicating a high infiltration rate in the limestone karst landscape. This agrees well with results from rainfall simulation in micro-plots which suggest that infiltration is high on most soil surface types under dry conditions. Macropores must be essential to explain both high instantaneous infiltration values and the very long times necessary to induce runoff.

Though the methods used in this study are not rigorous for the assessment of infiltration at different scales, they are complementary in explaining the different variables that control infiltration–runoff at micro-plot and slope scales. Joel et al. (2002) reported that the scale effect was a result of several interrelated factors, such as soil hydraulic conductivity, surface depressions, initial soil water content, slope length, crack development, and crusts and seal formation. For most events, the time and volume of rainfall per unit area required before runoff started were larger in large plots than in small ones. Eqs. (3) and (4) indicated that runoff generation at the hillslope scale was significantly correlated with rainfall intensity and depth and antecedent 20-day precipitation, which is in agreement with the results reported by Cammeraat (2004), showing that runoff only occurs at the highest scale level with very high rainfall intensity and large precipitation amounts. Our findings also confirm one of the main results of Frot et al. (2008), who stated that rainfall depth and the antecedent precipitation index over 20 days are the most influential factors in explaining runoff occurrence in the medium-size *aljibe* catchments in the same region and, additionally, rainfall intensity in the smaller ones. The Llano de los Juanes *aljibe* slope in this study, with a catchment of 9000 m², is close to and has a similar size to the smallest *aljibe* catchment in the region studied by Frot et al. (2008). The reasons that antecedent precipitation was a significant control on the hillslope (Eq. (3)) but antecedent soil moisture was not in the micro-plots (Eq. (1)) may be because rainfall intensity for slope under natural rainfall is 3.5 times lower than the simulated rainfall used at the micro-plots.

5. Conclusions

Two different and complementary approaches to characterise infiltration–runoff processes in a representative area of the Sierra de Gádor demonstrate that runoff is very low because of the high infiltrability of soils.

The spatial differences, assessed by rainfall simulations in micro-plots, stress the important role of vegetation as well as the presence of rock fractures as sinks of surface runoff in the limestone karst landscape, and the impact of the position of rock fragments on the infiltration of its soils. The ambivalent role of rock fragments in promoting runoff was also observed. Surfaces where rock fragments are resting on the soil, generally located in the middle of the slopes, prevent more efficiently the runoff generation than those surfaces where the rock fragments are embedded in the top soil (bottom of the dolines or hillslopes).

At the hillslope, natural rainfall characteristics (total depth and maximum hourly intensity per event) and antecedent precipitation over 20 days were the main variables explaining the runoff depth and coefficient. Runoff was rarely observed resulting in an overall infiltration of 41% of the total rainfall amount. The maximum infiltration rate was almost 94% of the largest single rainfall event.

The data presented here contribute to the understanding of the magnitude and controls of the surface runoff in the semiarid and calcareous (limestone and dolomites) Mountain areas surrounding the Mediterranean Basin. Additionally, this information complements other research results focused in assessing the recharge magnitude and the hydrological processes occurred in the Sierra de Gádor which is the main recharge area for the deep aquifers of Campo de Dalías.

Acknowledgements

We would like to thank anonymous reviewers for their valuable and constructive comments. The first author acknowledges the Spanish Ministry of Education and Science for his postdoctoral fellowship SB2000-0476. The second author enjoyed a postdoctoral fellowship (2008-0486) granted by the same Spanish institution in the framework of the National Program of Mobility of Human Resources (Plan I+D+I 2008–2011). This work was partially supported by research projects from the Spanish R+D programme, RECLISE (REN2002-045517-C02-02), CANOA (CGL2004-04919-C02-01), PROBASE (CGL2006-11619-HID), and the research project funded by Junta de Andalucía "Water balance in semiarid mountains" (P06-RNM1732), the National Key Technologies R&D Program (grant no. 2007BAC30B02) and the National Science Foundation of China (NSFC 40871025 and 41025001). Julien Sánchez, Alfredo Durán, and Montse Guerrero are acknowledged for their indispensable assistance in both field and laboratory work.

References

Abrahams, A.D., Parsons, A.J., 1991. Relation between infiltration and stone cover on a semiarid hillslope, southern Arizona. Journal of Hydrology 122, 49–59.

Arnau-Rosalén, E., Calvo-Cases, A., Boix-Fayos, C., Lavee, H., Sarah, P., 2008. Analysis of soil surface component patterns affecting runoff generation. An example of methods applied to Mediterranean hillslopes in Alicante (Spain). Geomorphology 101, 595–606.

Bergkamp, G., 1998. A hierarchical view of the interactions of runoff and infiltration with vegetation and microtopography in semiarid shrublands. Catena 33, 201–220.

Beven, K., 2002. Runoff Generation in Semi-arid Areas. In: Bull, L.J., Kirkby, M.J. (Eds.), Dryland Rivers: Hydrology and Geomorphology of Semi-arid Channels. John Wiley & Sons Ltd., Chichester, pp. 57–105.

Bowyer-Bower, T.A.S., 1993. Effects of rainfall intensity and antecedent moisture on the steady-state infiltration rate in a semi-arid region. Soil Use and Management 9, 69–76.

Calaforra, J.M., 2004. The Main Coastal Karstic Aquifers of Southern Europe: A Contribution by Members of the COST-621 Action 'Groundwater Management of Coastal Karstic Aquifers'. EU Publications Office. 123 pp.

Calvo-Cases, A., Boix-Fayos, C., Imeson, A., 2003. Runoff generation, sediment movement and soil water behaviour on calcareous (limestone) slopes of some Mediterranean environments in SE Spain. Geomorphology 50, 269–291.

Calvo-Cases, A., Boix-Fayos, C., Arnau-Rosalén, E., 2005. Patterns and Thresholds for Runoff Generation and Sediment Transport on Some Mediterranean Hillslopes.

In: García, C., Batalla, R. (Eds.), Catchment Dynamics and River Processes: Mediterranean and Other Climate Regions. Elsevier, Amsterdam, pp. 31–51.
Cammeraat, E.L.H., 2004. Scale dependent thresholds in hydrological and erosion response of a semi-arid catchment in southeast Spain. Agriculture, Ecosystems and Environment 104, 317–332.
Cantón, Y., Domingo, F., Solé-Benet, A., Puigdefábregas, J., 2002. Influence of soil surface types on the overall runoff of the Tabernas badlands (SE Spain). Field data and model approaches. Hydrological Processes 16, 2621–2643.
Cantón, Y., Villagarcía, L., Moro, M.J., Serrano-Ortíz, P., Were, A., Alcalá, F.J., Kowalski, A.S., Solé-Benet, A., Lázaro, R., Domingo, F., 2010. Temporal dynamics of soil water balance components in a karst range in southeastern Spain: estimation of potential recharge. Hydrological Sciences Journal 55, 737–753.
Cerdà, A., Ibáñez, S., Calvo, A., 1997. Design and operation of a small and portable rainfall simulator for rugged terrain. Soil Technology 11 (2), 161–168.
Contreras, S., 2006. Distribución espacial del balance hídrico anual en regiones montañosas semiáridas. Aplicación a Sierra de Gádor (Almería). PhD thesis, Universidad de Almería: Almería.
Contreras, S., Boer, M.M., Alcalá, F.J., Domingo, F., García, M., Pulido-Bosch, A., Puigdefábregas, J., 2008. An ecohydrological modelling approach for assessing long-term recharge rates in semiarid karstic landscapes. Journal of Hydrology 351, 42–57.
Duley, F.L., Domingo, C.E., 1943. Reducing the error in infiltration determination by means of buffer areas. Journal of the American Society of Agronomy 35 (7), 595–605.
Elías-Castillo, F., Ruiz-Beltrán, L., 1979. Precipitaciones Máximas en España. Estimaciones Basadas en Métodos Estadísticos. Monografías del ICONA, 21. Ministerio de Agricultura, Madrid.
Frot, E., van Wesemael, B., Sole-Benet, House, M.A., 2008. Water harvesting potential in function of hillslope characteristics: a case study from the Sierra de Gador (Almeria province, south-east Spain). Journal of Arid Environments 72, 1213–1231.
Horton, R.E., 1940. An approach toward a physical interpretation of infiltration capacity. Proceedings of Soil Science America Society 5, 399–417.
Imeson, A.C., Lavee, H., Calvo, A., Cerdà, A., 1998. The erosional response of calcareous soil along a climatological gradient in Southeast Spain. Geomorphology 24, 3–16.
Joel, A., Messing, I., Seguel, O., Casanova, M., 2002. Measurement of surface water runoff from plots of two different sizes. Hydrological Processes 16, 1467–1478.
Jones, D.P., Graham, R.C., 1993. Water-holding characteristics of weathered granitic rock in Chaparral and forest ecosystems. Soil Science Society of America Journal 57, 256–261.
Junta de Andalucía, 2005. Fotografía Aérea 0.5 m Resolución Espacial. Almería. DVD-Rom.
Lavee, H., Imeson, A.C., Pariente, S., Benyamini, Y., 1991. The Response of Soils to Simulated Rainfall Along a Climatological Gradient in an Arid and Semi-Arid Region. In: Bork, H.R., de Ploey, J., Schick, A.P. (Eds.), Erosion, Transport and Deposition Processes — Theories and Models: Catena Supplement, 19, pp. 19–37.
Lavee, H., Imeson, A.C., Sarah, P., 1998. The impact of climate change on geomorphology and desertification along a Mediterranean arid transect. Land Degradation and Development 9, 407–422.
Li, X.-Y., Contreras, S., Solé-Benet, A., 2007. Spatial distribution of rock fragments in dolines: a case study in a semiarid Mediterranean mountain-range (Sierra de Gádor, SE Spain). Catena 70, 366–374.
Li, X.-Y., Contreras, S., Solé-Benet, A., 2008. Unsaturated hydraulic conductivity in limestone dolines: influence of vegetation and rock fragments. Geoderma 145, 288–294.
Li, X.-Y., Yang, Z.-P., Li, Y.-T., Lin, H., 2009. Connecting ecohydrology and hydropedology in desert shrubs: stemflow as a source of preferential flow in soils. Hydrology and Earth System Sciences 13, 1133–1144.
Martin Rosales, W., 2002. Efecto de los diques de retención en el borde meridional de la Sierra de Gádor (Almería). PhD thesis, Universidad de Granada, Dep. Geodinámica. Granada. 266 p + 4 anexes.
Mayor, A.G., Bautista, S., Bellot, J., 2009. Factors and interactions controlling infiltration, runoff, and soil loss at the microscale in a patchy Mediterranean semiarid landscape. Earth Surface Processes and Landforms 34, 1702–1711.
Newman, B.D., Campbell, A.R., Wilcox, B.P., 1998. Lateral subsurface flow pathways in a semiarid ponderosa pine hillslope. Water Resources Research 34, 3485–3496.
Newman, B.D., Wilcox, B.P., Graham, R.C., 2004. Snowmelt-driven macropore flow and soil saturation in a semiarid forest. Hydrological Processes 18, 1035–1042.
Oyonarte, C. 1992. Estudio edáfico de la Sierra de Gádor (Almería). Evaluación para usos forestales, PhD thesis, Universidad de Granada, Granada.
Oyonarte, C., Escoriza, I., Delgado, R., Pinto, V., Delgado, G., 1998. Water-retention capacity in fine Herat and gravel fractions of semiarid Mediterranean montane soils. Arid Soil Research and Rehabilitation 12, 29–45.
Palmer, A., 1991. Origin and morphology of limestone caves. Geological Society of America Bulletin 103, 1–21.
Poesen, J., Ingelmo-Sanchez, F., 1992. Runoff and sediment yield from topsoils with different porosity as affected by rock fragment cover and position. Catena 19, 451–474.
Puigdefábregas, J., 2005. The role of vegetation patterns in structuring runoff and sediment fluxes in drylands. Earth Surface Processes and Landforms 30, 133–147.
Pulido-Bosch, A., Martín-Rosales, W., Vallejos, A., Molina, L., Navarrete, F., de Simón, E., 1993. The Southern Catchment Area of the Sierra de Gador and its Impact in the Campo de Dalias. In: Pulido-Bosch, A. (Ed.), Some Spanish Karstic Aquifers. Universidad de Granada, Granada, pp. 159–181.
Quinton, J.N., Edwards, G.M., Morgan, R.P.C., 1997. The influence of vegetation species and plant properties on runoff and soil erosion: results from a rainfall simulation study in south east Spain. Soil Use and Management 13, 143–148.
Seeger, M., 2007. Uncertainty of factors determining runoff and erosion processes as quantified by rainfall simulations. Catena 71, 56–67.
Solé-Benet, A., Calvo, A., Cerdà, A., Lázaro, R., Pini, R., Barbero, J., 1997. Influences of micro-relief patterns and plant cover on runoff related processes in badlands from Tabernas (SE Spain). Catena 31, 23–38.
StatSoft Inc., 2001. STATISTICA for Windows, computer program manual. Tulsa, OK, USA. http://www.statsoft.com.
Vahabi, J., Mahdian, M.H., 2008. Rainfall simulation for the study of the effects of efficient factors on run-off rate. Current Science 95, 1439–1445.
Vallejos, A., Pulido-Bosch, A., Martín-Rosales, W., Calvache, M.L., 1997. Contribution of environmental isotopes to the understanding of complex hydrological systems. A case study: Sierra de Gador, SE Spain. Earth Surface Processes and Landforms 22, 1157–1168.
van Wesemael, B., Poesen, J., Solé-Benet, A., Cara-Barrionuevo, L., Puigdefábregas, J., 1998. Collection and storage of runoff from hillslopes in a semi-arid environment: geomorphic and hydrologic aspects of the aljibe system in Almeria Province, Spain. Journal of Arid Environments 40, 1–14.
Vandenschrick, G., van Wesemael, B., Frot, E., Pulido-Bosch, A., Molina, L., Stiévenard, M., Souchez, R., 2002. Using stable isotope analysis (δD-$\delta^{18}O$) to characterise the regional hydrology of the Sierra de Gador, S-E Spain. Journal of Hydrology 265, 43–55.
Wilcox, B.P., 2002. Shrub control and streamflow on rangelands: a process based viewpoint. Journal of Range Management 55, 318–326.
Wilcox, B.P., Wood, M.K., Tromble, J.M., 1988. Factors influencing infiltrability of semiarid mountain slopes. Journal of Range Management 41 (3), 197–206.
Wilcox, B.P., Owens, M.K., Dugas, W.A., Ueckert, D.N., Hart, C.R., 2006. Shrubs, streamflow, and the paradox of scale. Hydrol Processes 20 (15), 3245–3259.
Wilcox, B.P., Wilding, L.P., Woodruff Jr., C.M., 2007. Soil and topographic controls on runoff generation from stepped landforms in the Edwards Plateau of Central Texas. Geophysical Research Letters 34, L24S24. doi:10.1029/2007GL030860.
Yair, A., 1996. Spatial Variability in Runoff in Semiarid and Arid Areas. In: Rubio, J.L., Calvo, A. (Eds.), Soil Degradation and Desertification in Mediterranean Environments. Geoforma, Logroño, pp. 71–90.
Yair, A., Lavee, H., 1985. Runoff Generation in Arid and Semi-Arid Zones. In: Anderson, M.G., Burt, T.P. (Eds.), Hydrological Forecasting. John Wiley and Sons, New York, pp. 183–220.